EFFECT OF DOPING ON TIME–OF–FLIGHT TRANSIENT CURRENTS IN THIN CRYSTALLINE LAYERS: A MONTE–CARLO STUDY

JAROSŁAW RYBICKI

Department of Solid State Physics,
Faculty of Technical Physics and Applied Mathematics,
Technical University of Gdansk, Narutowicza 11/12, 80–952 Gdansk, Poland,
and TASK Computer Centre, Narutowicza 11/12, 80–952 Gdansk, Poland
ryba@task.gda.pl

Abstract: In the paper we present the results of the Monte Carlo simulations of time–of–flight transient currents in hopping systems containing various concentrations of transport–active centres placed in an inert matrix, and doped with various concentrations of additional transport–active centres, characterised by a different ionisation potential than the host transport centres. Such hopping centre distribution can be found in molecularly doped organic crystals. The carriers are allowed to jump between localised states of two kinds: the host transport sites of concentration c_0, and the additional doping sites of concentration c_d. We deal only with the dependence of the carrier mobility on doping level, and on the difference of ionisation potentials between the host and dopant centres, at fixed external field and temperature. The results of simulations performed for various dopings, and various hopping sites distributions in energy, are discussed. The carrier jump statistics is discussed in detail.

Keywords: hopping transport, time–of–flight experiment, Monte Carlo methods

1. Introduction

In general, the increasing number of defects in crystals is accompanied by a decreasing carrier mobility. However, there are exceptions from this rule. For example, on doping of anthracene crystals with $\approx 1\%$ mol of 2,3–dimethylnaphtalene (DMN) the mobility increases in respect to the undoped crystals [2]. The phenomenon was explained by the authors in terms of antitraps. Marc *et al.* [5] studied the effect of doping molecules and addition of plasticizer on the carrier

mobility in poly–N–vinylcarbazole (PVK) photoconductors. In particular, the mobility of TNF–doped PVK, containing $0 \div 30\%$ wt of NPK, was investigated (here the abbreviations TNF and NPK stand for 2,4,7–trinitrofluorenone and N–phenyl-carbazole, respectively). In two more recent works by Wolf *et al.* [8] and Borsenberger *et al.* [1], studied hole trapping in tri–*p*–tolylamine–doped poly-styrene, and showed the appearance of the mobility minimum for certain dopant concentration, followed by the mobility increase for higher doping level.

One of the ways for determining the carrier mobility is the classical time–of–flight (TOF) experiment (*e.g.* [3], and references therein). In this experiment an infinitesimally thin sheet of charge carriers is produced near one of the surfaces of a thin layer, placed between two contacts, and subjected to an external electric field. The subsequent motion of the carriers towards the collecting contact results in a transient current which is analysed in an external circuit connected to the sample. There are two basic mechanisms of electronic transport in the bulk of non–ideal solids: multiple–trapping, and hopping. The first of them, the multiple–trapping mechanism, consists in the electron (or hole) band transport, interrupted repeatedly by the carrier trapping at the material imperfections (localised states, so called traps). Once trapped (temporarily immobilised) carrier is, after some random time, thermally activated to the band of extended states, where it participates again in the band transport. The hopping mechanism consists in the carrier jumps directly between localised states (tunnelling, or thermally activated tunnelling), without visiting the extended band states. In the present paper the hopping transport mechanism is taken into account.

The theory of the TOF experiment permits to perform an extensive analysis of the transient currents and to deduce a number of the layer transport parameters. However, there are no general analytical results describing the current profiles for arbitrary spatial and energetic distributions of hopping centres, and computer experiments, mainly Monte Carlo simulations, are often performed in order to elucidate specific features of current transients.

The present contribution is dedicated to a detailed Monte Carlo study of the mobility in hopping systems containing various concentrations of transport–active centres placed in an inert matrix, and doped with various concentrations of additional transport–active centres, characterised by a different ionisation potential than the host transport centres. The analysed model of a layer is guided by the experimental works on molecularly doped organic crystals referred to in the beginning of the paper. In the model the injected carriers are allowed to jump between localised states of two kinds: the host transport sites of concentration c_0, and the additional doping sites of concentration c_d. Here we deal with the dependence of the carrier mobility on doping level and on the difference of ionisation potentials between the host and dopant centres. All the results will refer to the fixed values of external field intensity, temperature, and layer thickness.

In Section 2 we remind in short the Monte Carlo algorithm that is usually applied in the simulations of the TOF transient currents, and describe in detail the model of

the layer that we have considered. The simulation results showing the TOF transient currents in their dependence on various model parameters are presented and discussed in Section 3. Section 4 contains concluding remarks.

2. Simulation algorithm

We consider a thin layer of thickness L placed between two planar contacts. At time $t = 0$ an infinitesimally thin sheet of carriers is generated on the contact at $x = 0$. The external electric field E (constant and uniform) enforces the carrier motion towards the $x = L$ contact. The carriers are allowed to hop between localised sites, distributed over the nodes of a simple cubic lattice, and distributed in energy ε, according to a given distribution $f(\varepsilon)$, with the average total (integrated over the energy) concentration c ($c = c_0 + c_d$).

The simulation system is similar to the one used by Ries and Bassler [6]: a regular cubic lattice of constant a, containing $M_x \times M_y \times M_z$ sites, with periodic boundary conditions imposed in directions perpendicular to the applied field. A fraction c of the total number of the lattice nodes are chosen as the hopping centres. The centre energies taken from a distribution $f(\varepsilon)$ are then assigned to the transport sites. The remaining fraction $1 - c$ of the lattice nodes is labelled as the host sites not participating in the transport process.

The transient currents were calculated from the time and spatial evolution of the injected carrier packet $n(x,t)$ during its motion towards $x = L$, according to the expression (*e.g.* [4]):

$$j(t) = \frac{1}{n_0} \frac{d}{dt} \left(\int_0^L n(x,t)dx \right) + \frac{1}{n_0 L} \frac{d}{dt} \left(\int_0^L xn(x,t)dx \right), \tag{1}$$

where $j(t)$ is the particle current density per one carrier, n_0 is the total number of injected carriers. The applied increment of $\log t$ was equal to 0.1 or 0.05. The carrier packets $n(x,t)$ were obtained by averaging the random walks of 3000 individual carriers (20 carriers for each of 150 site generations). The random walk of each individual carrier was started at $x = 0$ and $t = 0$, and finished on arriving to the collecting electrode at $x = L$.

An individual hop from a given occupied centre, say at $\mathbf{r}_0$, to one of the neighbouring empty centres, located at $\mathbf{r}_i$, $i = 1, \ldots, 342$ (from a $7a \times 7a \times 7a$ cube centred on $\mathbf{r}_0$), has been accomplished as follows. The average jump rate v_{0i} of a carrier localised at centre $\mathbf{r}_0$ to the i–th neighbouring empty centre at $\mathbf{r}_i$ is:

$$v_{oi} = \begin{cases} v_0 \exp(-2\alpha|\mathbf{r}_o - \mathbf{r}_i|) \cdot \exp(-\Delta U_{oi}/kT), & \Delta U_{oi} > 0, \\ v_0 \exp(-2\alpha|\mathbf{r}_o - \mathbf{r}_i|), & \Delta U_{oi} \leq 0, \end{cases} \tag{2}$$

where

$$\Delta U_{oi} = \varepsilon_i - \varepsilon_o - qE(x_i - x_o). \tag{3}$$

Here α is the reciprocal Bohr radius, ε_0 and ε_i are the energies of the actually occupied centre, and i–th neighbouring centre, v_0 is the frequency factor, q is the elementary charge, T is the temperature, and k is the Boltzmann constant. According to the average jump times $<t_{0i}> = v_0^{-1}$ random jump times are generated from an exponential distribution, and the shortest time is accepted.

The energetic centre distribution $f(\varepsilon)$ contains the host sites of mean energy ε_0, standard deviation σ, and concentration c_0 (a Gaussian distribution), and the doping sites of energy ε_d, and concentration c_d (a discrete energy level). ε_0 and ε_d, are distanced in energy by $\Delta\varepsilon$:

$$f(\varepsilon) = c_o g(\sigma, \varepsilon - \varepsilon_o) + c_d \delta(\varepsilon - \varepsilon_o - \Delta\varepsilon), \tag{4}$$

where g is the normalised Gaussian distribution, and δ is the Dirac function. In equation (4), c_0 is the concentration of transport sites in the absence of doping (host sites), and c_d is the concentration of the centres introduced on doping (guest sites), $0 \le c_d \le 1 - c_0$. The simulations have been performed for the systems with the following values of the parameters: the host centre concentration $c_0 = 0.5$ and $c_0 = 0.2$, the dopant concentration c_d in the whole range allowed by the model, *i.e.* $0.0 \le c_d \le 1 - c_0$. The energetic spacing $\Delta\varepsilon$ between ε_0 and ε_d was equal to 1/12, 1/6, 1/3, and 1/2 eV. The parameters common to all simulations are: the cubic lattice constant $a = 7 \cdot 10^{-10}$ m, the wave–function overlap parameter $2a\alpha = 5.0$, the external electric field $E = 1.1 \cdot 10^8$ V/m, the temperature $T = 400$ K. Thus, the host centre concentrations $c_0 = 0.5$ and $c_0 = 0.2$ correspond to about $1.46 \cdot 10^{27}$ m^{-3} and $0.58 \cdot 10^{27}$ m^{-3}. The σ parameter of the Gaussian distribution in energy was set to 0.0 (two discrete levels) or to 0.12 eV ($\sigma/kT = 3.5$). The time is normalised to $1/v = \tau$, where $v = 6 v_0 \cdot \exp(-2a\alpha)$. τ is the average dwell time of a carrier located at a site of undiluted ($c_0 = 1.0$) cubic lattice with six nearest neighbours, and for our data ($v_0 = 10^{13}$ Hz) equals to $0.2474 \cdot 10^{-11}$ s.

3. Simulation results and discussion

The increasing c_d increases the total centre density c, making the average inter–centre distance shorter. Consequently, the average tunnelling factor in equation (2) increases, and so the individual carrier jumps become easier. On the other hand, a finite energetic spacing $\Delta\varepsilon$ between the host and doping sites makes some of the jumps (from the deeper ε_d level to the ε_0 level) more difficult due to the Boltzmann factor. Thus, the appearance of the doping level influences the measured transient currents in a complicated way. In particular, even at fixed temperature and external electric field, the dependence of the current profiles on c_d should be qualitatively different for different densities of host centres c_0, and energetic spacing $\Delta\varepsilon$.

Let us consider in turn the doping level dependence of the shape of transient current profiles (Section 3.1), and of the effective time of flight and the slope of the final current decay (Section 3.2). Section 3.3 is dedicated to the carrier jump statistics.

3.1. Transient current profiles

Transient currents for two discrete energy levels will be discussed at first, and then the effect of continuous distribution of host centres will be described. For the both cases the host centre concentration c_0 is kept constant, and equals to 0.5. The only parameter being changed here is the doping level c_d, for various spacings $\Delta\varepsilon$: 1/12, 1/6, 1/3, and 1/2 eV. The curves in the figures showing transients currents are parametrised by the ratio $c_d' = c_d / (c_0 + c_d)$.

3.1.1. Two discrete energy levels

Figures 1–3 show several transient currents calculated for the energetic centre distribution (4) with $\sigma = 0.0$ eV, for various energetic differences $\Delta\varepsilon$ between the host centre level and doping centre level (1/12, 1/6, 1/3 eV in Figures 1, 2, 3, respectively).

At small spacing $\Delta\varepsilon$ (say $\Delta\varepsilon = 1/12$ eV) between shallower host sites and deeper doping sites, the current profiles hardly depend on the doping level in the range of $0.0 \leq c_d' \leq 0.2$ (Figure 1A). The effects due to the appearance of some activated jumps, and to the decrease of average tunnelling factor cancel each other. However, on increasing c_d, the increase of the average tunnelling factor prevails due to the increasing total transport centre concentration, and from $c_d' \approx 0.2$ on the conductivity increases with increasing doping (Figure 1B). Thus, the layer conductivity increases monotonously in the function of doping level, and reaches its maximum value for the highest dopant concentration allowed in the model ($c_d = 1 - c_0$). Curve e in Figure 1B was calculated for $c_0 = 1.0$ and $c_d = 0.0$. The difference between this curve and curve d ($c_0 = 0.5$, $c_d = 0.5$) results from the fact that in the latter case half of the centres differ in energy by $\Delta\varepsilon$ from the other centres. As it is seen, the shape of the current characteristic is not influenced by a small splitting of the centre energies, and leads only to a slightly lower effective carrier mobility.
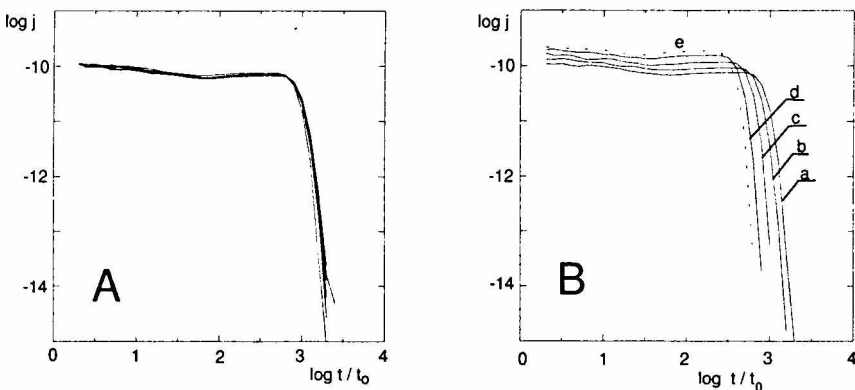

Figure 1. *The dependence of the transient current profiles on the normalised doping level c_d'. $c_0 = 0.5$, $\Delta\varepsilon = 1/12$ eV, $\sigma = 0.0$ eV. Figure A: overlapping transient currents calculated for $c_d' = 0.0$, 0.025, 0.05, 0.075, 0.1, 0.15, and 0.2; Figure B: curve a: $c_d' = 0.2$; curve b: $c_d' = 0.3$; curve c: $c_d' = 0.4$; curve d: $c_d' = 0.5$; curve e: $c_0 = 1.0$, $c_d' = 0.0$*

The dependence of transient currents on doping level becomes much more complicated for higher values of $\Delta\varepsilon$. Figure 2 shows the currents calculated for the same parameters as in Figure 1, but for a doubled value of level splitting, $\Delta\varepsilon$ = 1/6 eV. Here even a fairly low doping level causes a significant change in the characteristics shape (Figure 2A). In the range of $0.0 < c_d' \leq 0.1$ the effective time of flight increases with increasing c_d and the transient consists of two stages: the current decrease due to carrier trapping (downward jumps into dopant centres), and a constant–current fragment, corresponding to the transport in conditions of thermal equilibrium between the centres of energies ε_0 and $\varepsilon_0 + \Delta\varepsilon$. The only exception is curve b in Figure 2A, calculated for the lowest doping level, $c_d' = 0.025$. For the dimensions of the simulation box used here, the time scale of the first trapping events is comparable with the effective time of flight, so that thermal equilibrium could not be achieved, and the horizontal fragment of the characteristic is absent. Here the carriers during their random walk towards $x = L$ interact only a few times with dopant centres. In the range of $0.1 < c_d' \leq 0.2$ the shape of the characteristics only weakly depends on c_d, although the hop statistics systematically changes (Section 3.3). For $c_d' > 0.2$ (Figure 2B) the transport channel related to direct jumps between dopant centres becomes operative, what leads to the effective mobility increase. It should be noted, that in this particular case ($c_0 = 0.5$), the transient currents in undoped ($c_d = 0.0$), and in the maximally doped ($c_d = 0.5$) layers are identical. In the latter case the carriers started at $x = 0.0$ on the ε_0 level immediately fall into the $\varepsilon_0 + \Delta\varepsilon$ centres, and move towards the collecting electrode jumping only between the dopant sites. Obviously, for $c_0 < 0.5$ the conductivity at the maximum doping $(1 - c_0)$ is higher than in an undoped layer.
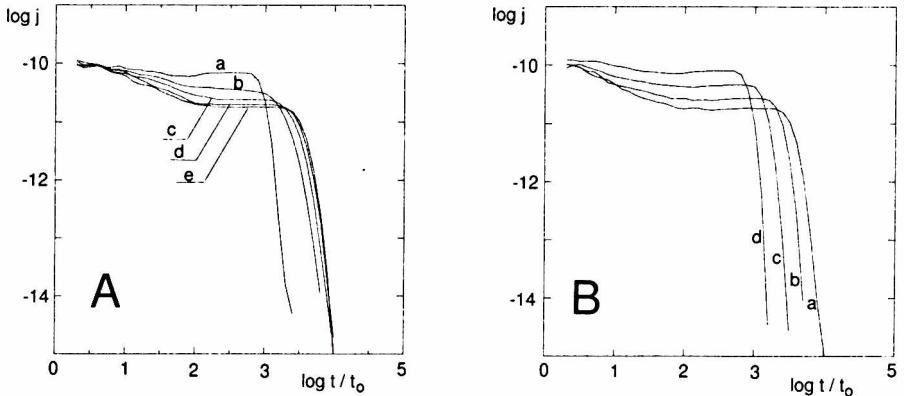

Figure 2. *The dependence of the transient current profiles on the normalised doping level c_d'. $c_0 = 0.5$, $\Delta\varepsilon = 1/6$ eV, $\sigma = 0.0$ eV. Figure A: curve a: $c_d' = 0.0$; curve b: $c_d' = 0.025$; curve c: $c_d' = 0.05$; curve d: $c_d' = 0.075$; curve e: $c_d' = 0.1$; Figure B: curve a: $c_d' = 0.2$; curve b: $c_d' = 0.3$; curve c: $c_d' = 0.4$; curve d: $c_d' = 0.5$. Curve d in Figure B is identical to curve a in Figure A, for $c_d = 0.0$*

For still greater difference $\Delta\varepsilon$ ($\Delta\varepsilon = 1/3$ eV, Figure 3), the initial carrier trapping leads to more pronounced decrease of the current at early times in respect to the current initial value, and the absorption edge is more abrupt. We have calculated
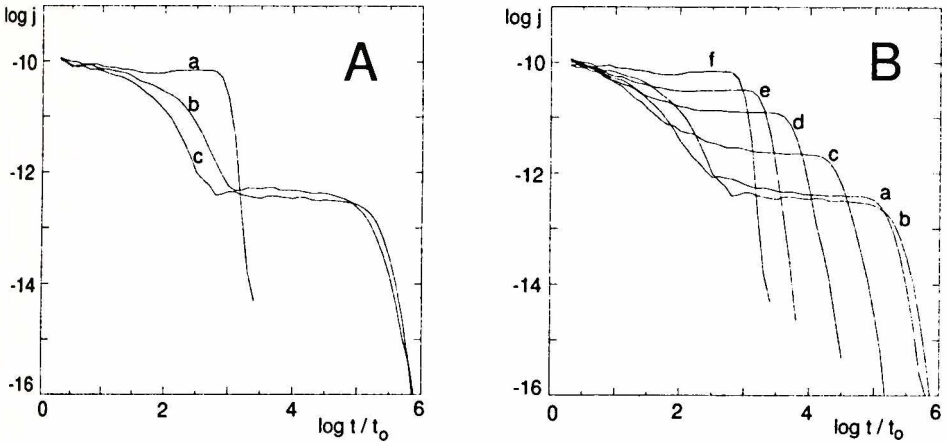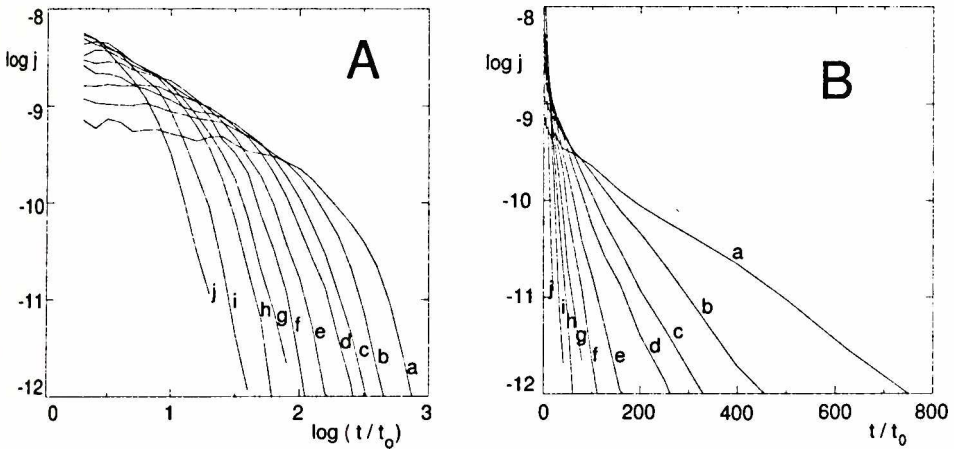
Figure 3. *The dependence of the transient current profiles on the normalised doping level c_d' . $c_0 = 0.5$, $\Delta \varepsilon = 1/3$ eV, $\sigma = 0.0$ eV. Figure A: curve a: $c_d' = 0.0$; curve b: $c_d' = 0.025$; curve c: $c_d' = 0.05$; Figure B: curve a: $c_d' = 0.05$; curve b: $c_d' = 0.1$; curve c: $c_d' = 0.2$; curve d: $c_d' = 0.3$; curve e: $c_d' = 0.4$; curve f: $c_d' = 0.5$. Curve f in Figure B is identical to curve a in Figure A, calculated for $c_d = 0.0$*

Figure 4. *Absorbtion currents in the function of dopant concentration c_d'. Dopant centres act here as infinitely deep traps. Host centre concentration $c_0 = 0.5$. Curves a: $c_d' = 0.025$; curves b: $c_d' = 0.05$; curves c: $c_d' = 0.075$; curves d: $c_d' = 0.1$; curves e: $c_d' = 0.15$; curves f: $c_d' = 0.2$; curves g: $c_d' = 0.25$; curves h: $c_d' = 0.3$; curves i: $c_d' = 0.4$; curves j: $c_d' = 0.5$. A: log–log scale; B: log–lin scale*

pure absorption currents, *i.e.* the currents obtained at the same parameters as in Figure 3, but the random walk of each carrier was here stopped on the first interaction with a dopant site. Such absorption currents (Figure 4) were proportional to $\exp(-t'/\tau_a)$, where $t' = t/t_0$. Absorption constants τ_a are shown in Figure 5A ($\bullet$ — line). As it is seen from Figures 2–4 and 5A, the time extension of initial current decay is directly related to the first–trapping–time. Figure 5A shows also distribution of times at which the first encounter with doping centre takes place for various concentrations c_d ($\circ$ — line). The first–trapping times, t_1, are distributed approximately according to an exponential low, $t_1 \propto \exp(-t/\tau_1)$, where τ_1 depends on c_d. τ_1 is the average life–time of the carriers in the upper centre fraction. Figure 6
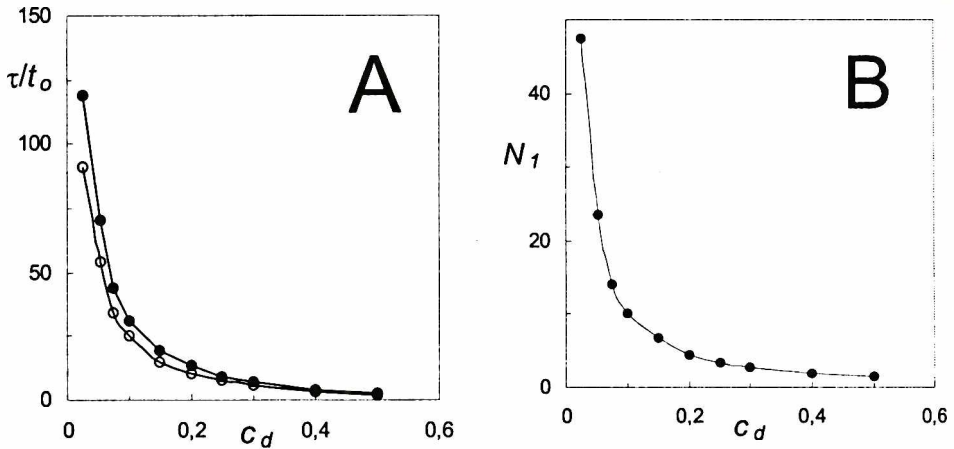
Figure 5. Dependence of τ_a (•) and τ_1 (○) times on c_d (A), and dopant concentration dependence of N_1 constants (B)
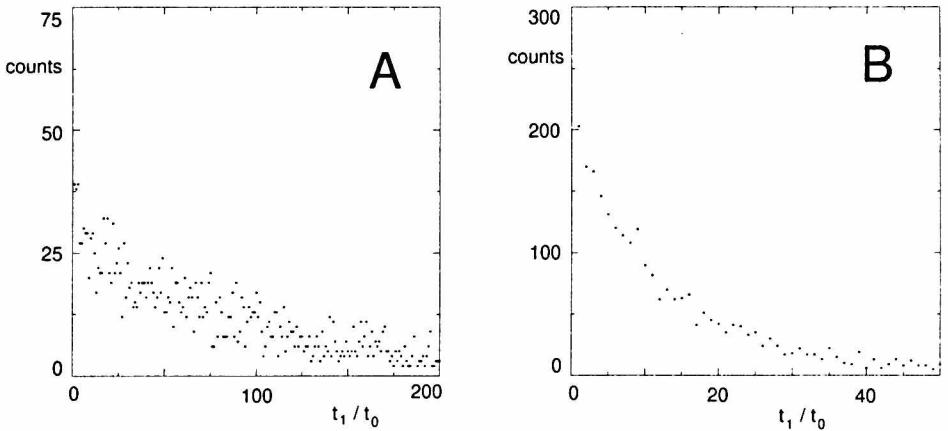

Figure 6. Distribution of t_1 times for various concentrations c_d' for $c_0 = 0.5$; (A) $c_d' = 0.025$; (B) $c_d' = 0.15$
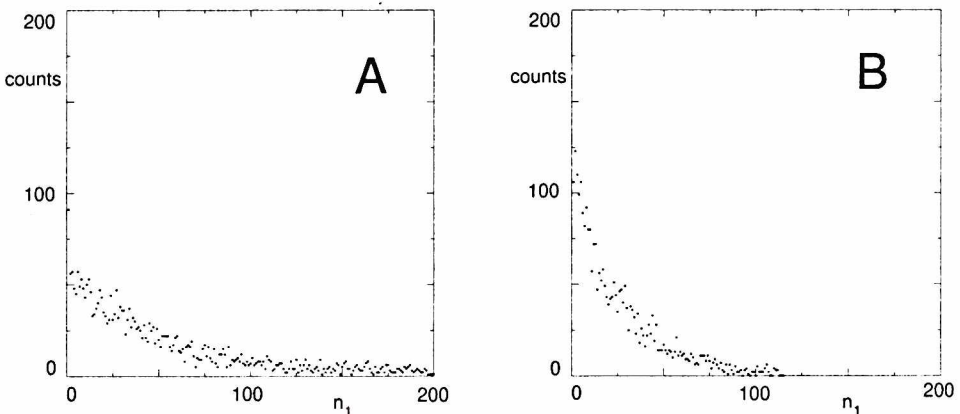

Figure 7. Distributions of n_1 values for two doping levels: $c_d' = 0.025$ (A), and $c_d' = 0.05$ (B). $c_0 = 0.5$

shows exemplary distributions of times t_l for various concentrations c_d. The numbers of hopping events, n_1, after which the absorption occurs, are distributed exponentially (Figure 7): $n_1 \propto \exp(-n_l / N_1)$. The c_d — dependence of N_1 is shown in Figure 5B.

3.1.2. Discrete doping level added to Gaussian host centre distribution

A discrete doping level introduced into a layer characterised by a Gaussian energetic distribution modifies the shape of transient currents generally in a similar way as discussed in the previous section. However, despite of many similarities some remarkable differences are to be noted. For $\Delta\varepsilon < \sigma$ (Figure 8A, $\Delta\varepsilon = 1/12$ eV) the increase of the conductivity occurs even at extremely low doping level, in contradistinction to the case of two discrete energy levels (*cf.* Figure 1). The monotonous increase of the conductivity in the function of increasing doping is also observed for $\Delta\varepsilon \approx \sigma$ (Figure 8B, $\Delta\varepsilon = 1/6$ eV), where no absorption effects can be distinguished in the shape of the current characteristics, and where no current–insensibility range of c_d exists (*cf.* Figure 2). For the level splitting $\Delta\varepsilon \leq \sigma$ the slope of the final current decay is only weakly c_d — dependent. The absorption effects related to the first–trapping events become visible for $\Delta\varepsilon > \sigma$. In systems with wider energetic distribution of host centres ($\Delta\varepsilon \geq 1/3$ eV) the qualitative dependence of the shape of transient currents becomes similar to the one shown in Figures 2 and 3.
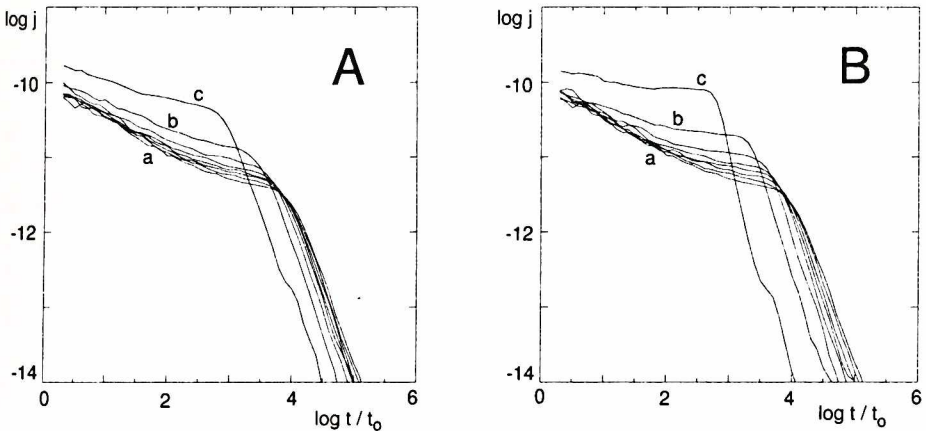

Figure 8. The dependence of the transient current profiles on the normalised doping level c_d' .Host centre concentration $c_0 = 0.5$, $\sigma = 0.12$ eV. Figure A: $\Delta\varepsilon = 1/12$ eV; curve a: $c_d' = 0.0$; curve b: $c_d' = 0.25$; curve c: $c_d' = 0.5$; Figure B: $\Delta\varepsilon = 1/6$ eV; curve a: $c_d' = 0.0$; curve b: $c_d' = 0.25$; curve c: $c_d' = 0.5$. Between curves a and b the transients calculated for $c_d' = 0.025, 0.05, 0.075, 0.1$, and 0.15 are also shown

3.2. Effective time–of–flight and slope of the final current decay

The simulation results obtained for $c_0 = 0.5$ (discussed in the preceding section), and also for $c_0 = 0.2$ (with the maximum doping level $c_d = 0.8$) are summarised in terms of the effective time–of–flight, and of the slope of the final current decay in

Figures 9 and 10. In particular, Figure 9 shows the dependence of the effective time of flight on doping level c_d ($0.0 \leq c_d \leq 1 - c_0$) for various values of the energy difference $\Delta\varepsilon$, for the cases of a discrete host sites energy (Figures 9A, and 9C), and a Gaussian distribution of the host sites energies (Figures 9B and 9D). In each case for a sufficiently small value of $\Delta\varepsilon$ the effective time–of–flight decreases with increasing doping level, so that the conductivity calculated from the effective time–of–flight increases with doping. For larger differences $\Delta\varepsilon$, the dependence of the conductivity on the doping level becomes more complicated: it initially decays with c_d, reaches its minimum (maximum of the effective time–of–flight) at a certain doping level c_{d0}, which depends on $\Delta\varepsilon$, and for higher dopant concentrations increases continuously to its maximum value. For the fixed c_0 the critical doping level c_{d0}, corresponding to the minimum of the conductivity, decreases with increasing $\Delta\varepsilon$, and this dependence is stronger for lower c_0 and/or narrower distribution of host centres σ. Finally, for still greater $\Delta\varepsilon$'s, the doping centres act as absorption centres, and only exponential current decay would be observed, with no defined effective time–of–flight (for sufficiently thick layers).

The slope of the final (for times exceeding the effective time–of–flight) current decay in the log–log coordinates is another important characteristics of transient currents. It is a simple and direct measure of the degree of the transport dispersion. Figure 10 shows the absolute values of the final current slopes $-\beta - 1$, as a function of the doping level. $\beta = 0$ corresponds to the high dispersion limit, whereas $\beta = \infty$ indicates no dispersion at all. Parameter β, calculated from our MC results, depends on c_d in a quite different way for a discrete, and a sufficiently wide continuous host centre distribution in energy. In particular, for a discrete host centre level, the dispersion degree assumes its maximum value at the doping levels slightly lower than c_{d0} (curves b, c, d in Figure 10A), and the dispersion maximum appears even if no conductivity minimum is observed (curve a in the same figure). Moreover, the final current decay depends significantly on the doping level also for the smallest $\Delta\varepsilon$ we have considered. On the contrary, for a finite width of the host centre energetic distribution, no dispersion maxima in the function of doping level are observed. At lower spacings $\Delta\varepsilon$, the dispersion degree remains almost independent of c_d, whereas in the structures with larger σ the dispersion decreases monotonously with increasing doping (approximately from $c_d \approx c_0$ on). In general, the currents become steeper in the post time–of–flight region with increasing doping, and/or with decreasing width of the host centre distribution in energy. Such behaviour can be related to the carrier jump statistics, which is discussed in the subsequent section.

3.3. Carrier jump statistics

One of the advantages of the Monte Carlo computer simulations consists in a facility to monitor the quantities inaccessible in a real experiment as, for instance, the carrier hop statistics. Figures 11, and 12 show the histograms of the total number of jumps the individual carriers performed between $x = 0.0$ and $x = L$ for several transients shown in Figures 1, and 3, respectively. At low spacing $\Delta\varepsilon$, (Figure 11,
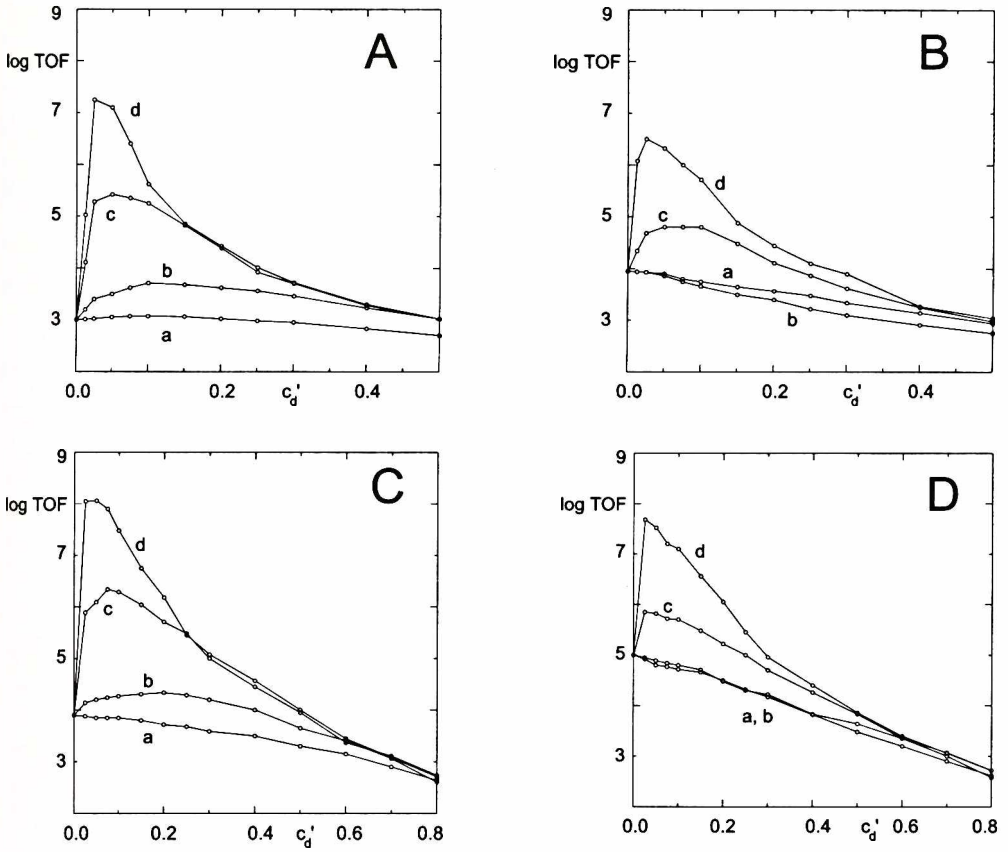
Figure 9. *The dependence of the effective time–of–flight on the normalised doping level c_d' for various values of $\Delta\varepsilon$. Figure A: $\sigma = 0.0$ eV, $c_0 = 0.5$; Figure B: $\sigma = 0.12$ eV, $c_0 = 0.5$; Figure C: $\sigma = 0.0$ eV, $c_0 = 0.2$; Figure D: $\sigma = 0.12$ eV, $c_0 = 0.2$. Curves a: $\Delta\varepsilon = 1/12$ eV; curves b: $\Delta\varepsilon = 1/6$ eV; curves c: $\Delta\varepsilon = 1/3$ eV; curves d: $\Delta\varepsilon = 1/2$ eV*
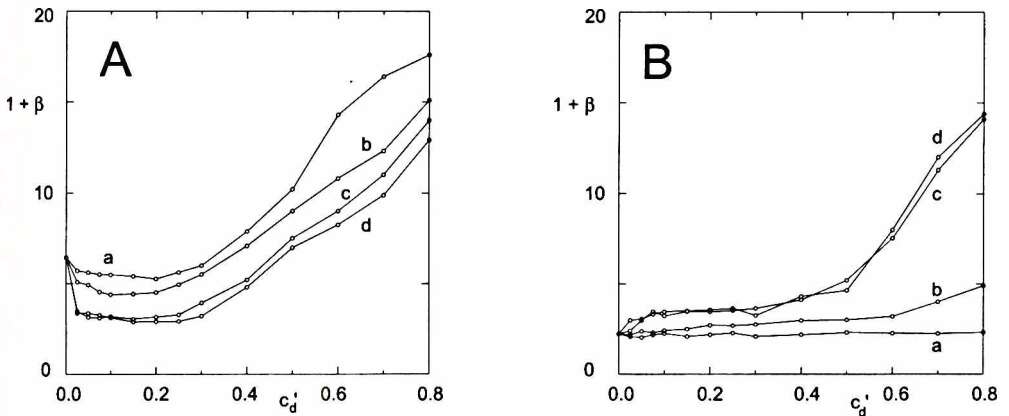

Figure 10. *Absolute values of slopes of the final current decay in their dependence on the normalised doping level c_d'. Figure A: $\sigma = 0.0$ eV, Figure B: $\sigma = 0.12$ eV. Host centre concentration $c_0 = 0.2$. Curves a: $\Delta\varepsilon = 1/12$ eV; curves b: $\Delta\varepsilon = 1/6$ eV; curves c: $\Delta\varepsilon = 1/3$ eV; curves d: $\Delta\varepsilon = 1/2$ eV*

$\Delta\varepsilon = 1/12$ eV) the distribution of the total number of jumps of the individual carriers depends on the doping level monotonously, and rather weakly. Figures 11A and 11B show the distributions for the two limiting values of c_d' (0.0 and 0.5, respectively). On increasing c_d' , the average number of hops necessary to reach the collecting electrode decreases, and their dispersion about the average value also decreases. A similar hop distribution calculated for $c_d = 0.0$ and $c_0 = 1.0$ (curve e in Figure 1B) has the same shape as the distribution showed in Figure 8B, but is slightly shifted to the right (towards higher jump numbers). Since the effective time of flight in the layer characterised by $c_d = 0.0$, $c_0 = 1.0$ is shorter than in the layer characterised by $c_d = 0.5$, $c_0 = 0.5$, it follows that the average jump time is shorter in the former case. At higher values of $\Delta\varepsilon$ the distribution of total numbers of jumps depends on the doping level much more rapidly, and in a qualitatively different way. Figure 12 presents a sequence of histograms for several values of c_d' in the range of 0.025 ÷ 0.3, for $\Delta\varepsilon = 1/3$ eV and $c_0 = 0.5$ (cf. Figure 3). As it is seen, even at a fairly low doping level (0.025) there appears a long tail of carriers, which between $x = 0.0$ and $x = L$ perform many more hops than on average (Figure 12A). With increasing doping level c_d the distribution evolves in a complicated way. The most probable number of jumps moves to the higher values, and the distribution becomes always wider up to c_d' ≈ 0.1. In this doping range the conductivity decreases, whereas the dispersion degree increases. For higher values of c_d' , the most probable number of hops systematically decreases, and the distribution becomes narrower again.
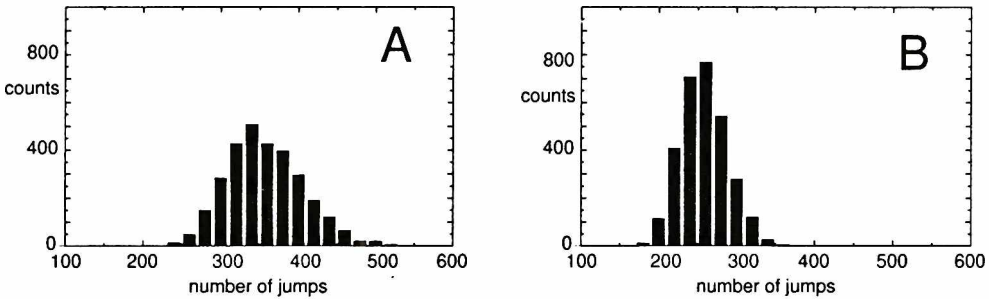

Figure 11. Histograms of the numbers of jumps performed by the carriers between x = 0.0 and x = L. Centre distribution (4), c_0 = 0.5, $\Delta\varepsilon$ = 1/12 eV. Figure A: c_d' = 0.0; Figure B: c_d' = 0.5

Several types of jumps contribute to their total number. These are: a) jumps between two host sites (h → h); b); jumps between two dopant sites (d → d); c) jumps from a host site to a dopant site (h → d); d) jumps from a dopant site to a host site (d → h). Figure 13 shows the relative (%) contribution of h → h, d → d, h → d and d → h jumps to the total number of hops in the function of the doping level c_d for various values of $\Delta\varepsilon$. For smaller distances $\Delta\varepsilon$ (1/12, and 1/6 eV, Figures 13A, and 13B) at a low doping level the h → h jumps dominate, the d → d jumps are almost absent, and there are few h → d, and d → h transitions. On increasing doping the contribution of the h → h jumps decays, and the direct d → d
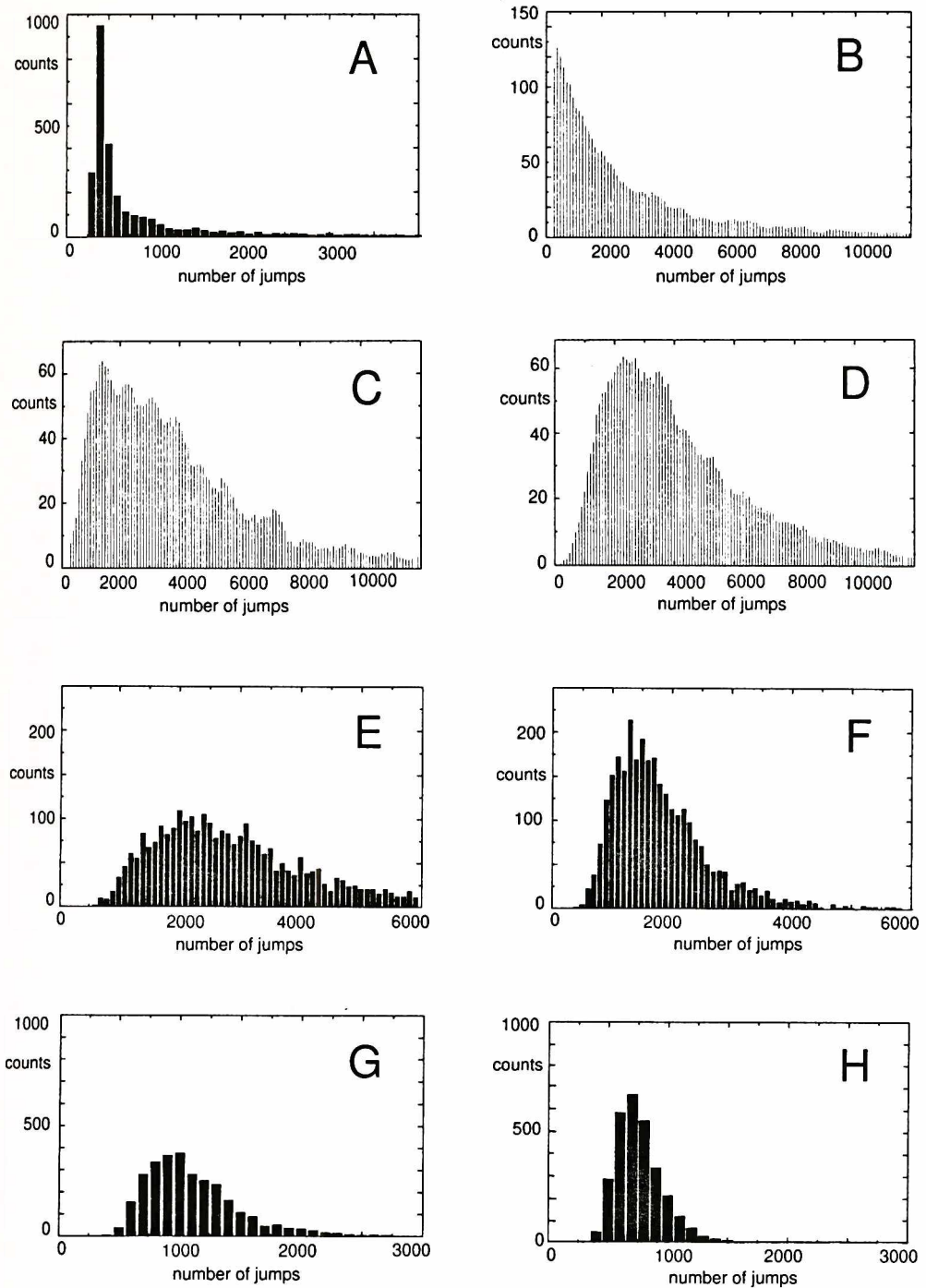
Figure 12. *Histograms of the numbers of jumps performed by the carriers between x = 0.0 and x = L. σ = 0.0, c_0 = 0.5, Δε = 1/3 eV. Figure A: c'_d = 0.025; Figure B: c'_d = 0.05; Figure C: c'_d = 0.075; Figure D: c'_d = 0.1; Figure E: c'_d = 0.15; Figure F: c'_d = 0.2; Figure G: c'_d = 0.25; Figure H: c'_d = 0.3.*

jumps turn to be dominant for sufficiently high c_d. At the same time the contribution of the h → d, and d → h transitions increases, obtaining its maximum at the dopant concentration for which the h → h, and d → d transitions are equally probable. It should be noted, that the h → d, and d → h transitions are equally probable, so we have an equilibrium transport. For greater distances $\Delta\varepsilon$ (1/3, and 1/2 eV, Figures 13C, and 13D) at a low doping level the d → d jumps prevail even at the lowest doping levels considered. The h → h jumps disappear at fairly low dopings. Also the contribution of the h → d, and d → h transitions readily becomes negligible. Within the time scale of the experiment the thermal equilibrium between the host and dopant centres is not achieved: there are more downward jumps than the upwards ones (curves c, and d in Figures 13C, and 13D). Because of a poor statistics we can not extract any unambiguous conclusions on the detailed dependence of the relative contributions of the h → h, h → d, and d → h transitions on c_d' for high spacings $\Delta\varepsilon$ (curves a, c, and d in Figure 13D).
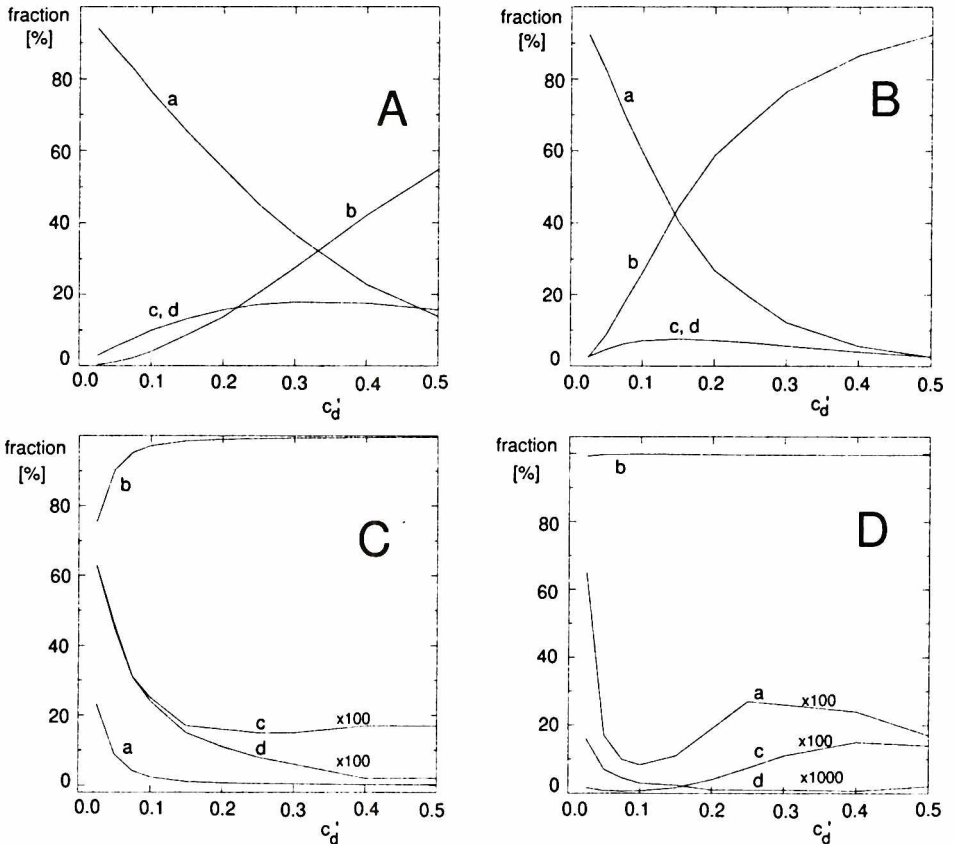

Figure 13. *Relative (%) contribution of various jump types in total number of jumps between x = 0.0 and x = L in their dependence on c_d'. Curves a: jumps h → h; curves b: jumps d → d; curves c: jumps h → d; curves d: jumps d → h. Figure A: $\Delta\varepsilon = 1/12$ eV, Figure B: $\Delta\varepsilon = 1/6$ eV, Figure C: $\Delta\varepsilon = 1/3$ eV, Figure D: $\Delta\varepsilon = 1/2$ eV. $c_0 = 0.5$*

Figure 14 shows how the average number of the h → h, and d → d jumps per one carrier depends on c_d for various Δε. The average number of the h → h transitions per one carrier decreases monotonously with c_d for all values of Δε, the decrease being obviously more rapid at higher energetic spacings Δε (Figure 14A). The average number of the d → d jumps increases monotonously with the doping level only for sufficiently small spacing Δε, whereas for greater Δε's a maximum appears at a certain c_d, not related directly to the dopant concentration corresponding to the minimum conductivity at c_{d0}. Great numbers of the d → d transitions appearing in Figure 14B at dopant concentrations 0.1, and 0.05 for Δε equal to 1/3, and 1.2 eV, respectively, result from repeated quick jumps within isolated doping centre clusters, and not imply the overall conductivity decrease.
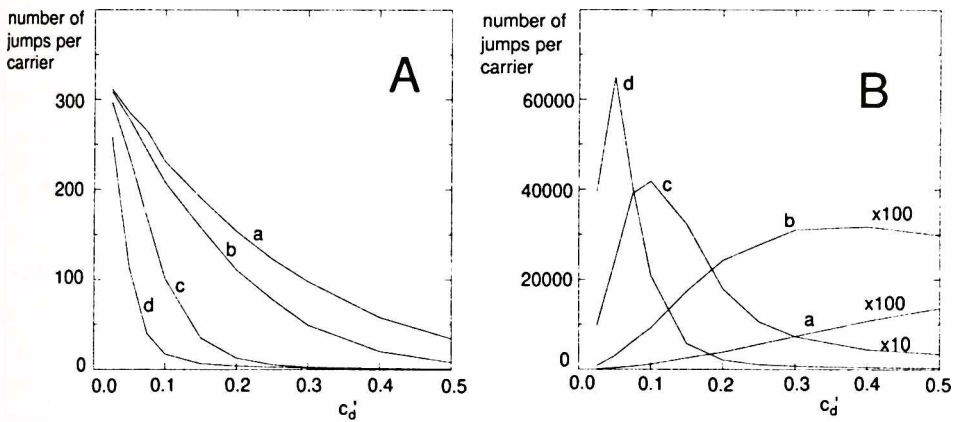

Figure 14. *Average number of jumps of various types of transitions per one carrier during its walk to the collecting electrode in dependence on doping level c_d' for various values of Δε. Curves a: Δε = 1/12 eV, curves b: Δε = 1/6 eV, curves c: Δε = 1/3 eV, curves d: Δε = 1/2 eV. Figure A: h → h jumps, Figure B: d → d jumps. Host centre concentration $c_0 = 0.5$*

4. Concluding remarks

We have discussed the hopping transport TOF current profiles in thin layers containing two fractions of localised centres: host centres, and doping centres, distanced in energy by Δε. The calculations were performed using the Monte Carlo method. Attention has been paid to the current dependence on the centre concentration and on Δε at a fixed external electrical field and temperature, and the typical values of parameters like the Bohr radius, or the frequency coefficient have been used. It has been shown that within our model the layer conductivity in a wide range of parameters initially decreases on increasing doping, assumes its minimum value, and then again increases for still increasing doping level.

It should be noted, that although the increase of Δε by a certain factor p is equivalent to the decrease of the temperature by the same factor with unchanged Δε, the results presented above for various Δε's can not be simply translated to various temperatures (*cf.* formula (2)). The temperature dependence of

current transients, although in general qualitatively similar to the dependence on $\Delta\varepsilon$ is more complicated, and to some extent has been discussed elsewhere [7].

In the present paper we have considered transport in systems containing two different fractions of localised centres. If the upper energy level is well distanced from the conductivity band, only direct jumps between the centres are possible, and one can consider the pure hopping transport. On the other hand, if the upper level is close to the bottom of the conductivity band, both the hopping transport channel, and the multiple–trapping transport channel can be simultaneously active, at least in certain temperature ranges. Such a situation probably exists in hydrogen reduced oxide glasses [7]. MC simulations of transients for this case are in progress.

Acknowledgement

References

[1] Borsenberger P M, Gruenbaum W T, Wolf U i Bassler H 1997 *Chem. Phys.* **234** 277
[2] Emoto N and Kotani M 1983 *Chem. Phys. Lett.* **101** 386
[3] Kao K C and Hwang W 1981 *Electrical Transport in Solids,* Oxford, Pergamon
[4] Leal Ferreira G F 1977 *Phys. Rev.* B **16** 4719
[5] Marc N, Moisan J Y. Andre B and Lever R 1996 *Phil. Mag.* B **74** 93
[6] Ries B and Bassler H 1987 *Phys. Rev.* B **35** 2295
[7] Rybicki J, Trzebiatowski K, Witkowska A and Feliziani S 1998 *Proc. Int. Symp. on Trends in Continuum Physics*, TRECOP'98, August 17–20, Poznań, Poland)
[8] Wolf U, Bassler H, Borsenberger P M i Grunebaum W T 1997 *Chem. Phys.* **222** 259